


Lifetimes of the Metastable $6d^2D_{5/2}$ and $6d^2D_{3/2}$ State of Ra^+

Haoran Li^{*}, Huaxu Dan[✉], Mingyu Fan[✉], Spencer Kofford[✉], Robert Kwapisz[✉], Roy A. Ready[✉], Akshay Sawhney[✉],
Merrell Brzeczczek[✉], Craig Holliman[✉], and Andrew M. Jayich[✉]
Department of Physics, *University of California, Santa Barbara*, California 93106, USA

S. G. Porsev[✉]
Department of Physics and Astronomy, *University of Delaware*, Newark, Delaware 19716, USA

M. S. Safronova^{✉†}
Department of Physics and Astronomy, *University of Delaware*, Newark, Delaware 19716, USA
and Joint Quantum Institute, *National Institute of Standards and Technology* and
the University of Maryland, College Park, Maryland 20742, USA

 (Received 31 January 2025; revised 22 May 2025; accepted 5 June 2025; published 11 August 2025)

We report lifetime measurements of the metastable $6d^2D_{5/2}$ and $6d^2D_{3/2}$ states of Ra^+ . The measured lifetimes, $\tau_5 = 303.8(1.5)$ ms and $\tau_3 = 642(9)$ ms, are important for optical frequency standards and for benchmarking high-precision relativistic atomic theory. Independent of the reported measurements, the D state lifetimes were calculated using the coupled-cluster single double triple method, in which the coupled-cluster equations for both core and valence triple excitations were solved iteratively. The method was designed for precise prediction of atomic properties, especially for heavy elements, where relativistic and correlation corrections become large, making their treatment more challenging. This Letter presents the first tests of the method for transition properties. Our prediction agrees with experimental values within the uncertainties. The ability to accurately predict the atomic properties of heavy elements is important for many applications, from tests of fundamental symmetries to the development of optical clocks.

DOI: [10.1103/5754-4cbv](https://doi.org/10.1103/5754-4cbv)

The radioactive elements at the bottom of the periodic table are intriguing both for science and technology [1]. However, many isotopes are challenging for experimentation due to their short half-lives. Therefore, accurate theoretical predictions of transition frequencies and electronic state lifetimes can provide helpful guidance for experiments. But unfortunately the large atomic numbers of heavy elements make accurate calculations notoriously difficult because of both electron correlations and relativistic effects. To accurately calculate their properties the coupled-cluster single double triple method (CCSDT) was developed [2]. It was applied to extract nuclear moments from the hyperfine structure of ^{229}Th in [2]. Here, we present the first test of this approach comparing the *ab initio* theoretical values with experimental results of the metastable D state lifetimes of Ra^+ .

We report a precision measurement of the $6d^2D_{5/2}$ state lifetime of Ra^+ , $\tau_5 = 303.8(1.5)$ ms, improving on a previous lower bound, $\tau_5 \geq 232(4)$ ms [3], and the first measurement of the $6d^2D_{3/2}$ state lifetime, $\tau_3 = 642(9)$ ms, see Fig. 1. The measurement precision is sufficient to support a test between experiment and the

CCSDT theory predictions, which were estimated to be accurate to 1%.

The metastable D states of Ra^+ both support optical clock transitions. The radium ion is appealing for optical clocks both for achieving very high precision and for realizing transportable devices [4]. Its high mass and low charge to mass ratio reduce leading systematic uncertainties arising from the second-order Doppler effect [5]. With $^{225}Ra^+$ (nuclear spin $I = 1/2$) for both the $S_{1/2} \leftrightarrow D_{5/2}$ and $S_{1/2} \leftrightarrow D_{3/2}$, there are transitions which are first-order insensitive to magnetic field noise and both support optical clocks. Because of the large hyperfine structure of $^{225}Ra^+$ it is possible to operate an optical clock with only laser light at 828 and 1079 nm using the $S_{1/2} \leftrightarrow D_{3/2}$ transition for the clock [6]. Requiring only low-power IR light could facilitate the use of integrated photonics that would help enable a transportable clock. Knowledge of both lifetimes is important for calculating clock performance.

In the theoretical calculations, we took into account triple excitations and nonlinear (NL) terms, evaluated the contribution of higher partial waves, and computed smaller effects such as the Breit interaction and quantum electrodynamical corrections. Both core and valence triple excitations were included on the same footing as single and double excitations, i.e., iteratively solving the equations for

^{*}Contact author: hli836@ucsb.edu

[†]Contact author: msafro@physics.udel.edu

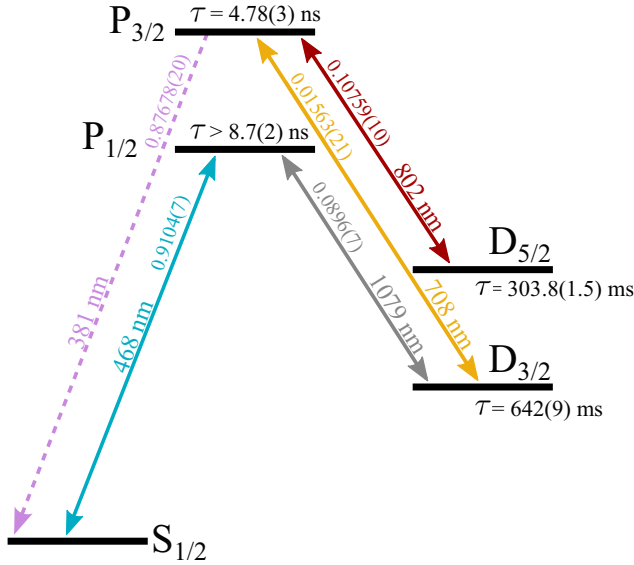


FIG. 1. Low-lying Ra^+ level structure, with experimentally measured branching ratios and lifetimes [9–12]. The solid lines indicate the transitions driven in this measurement.

triple cluster amplitudes. The NL terms were included in the equations for single and double excitations. This approach represents the most accurate treatment of electronic correlations in heavy systems.

This new method allowed us to reduce the uncertainty of the matrix elements $\langle 7s^2S_{1/2} || Q || 6d^2D_{3/2,5/2} \rangle$ to the level of 0.5%. Performing several calculations with increasing complexity enables us to put an uncertainty bound on our values. Comparing the theoretical results with the precision measurements carried out in this Letter, we observe an excellent agreement, confirming not only the validity of our approach but also our estimate of theory uncertainty, which is crucial for the other cases where experiments are not yet available. This is a good test of our CCSDT approach for transition matrix elements and lifetimes, which are determined by the quality of the wave functions at a large distance from the nucleus.

We note that accurate prediction of actinide properties is a very challenging task because of substantial core-valence correlations that need to be treated with a higher level of precision compared to lighter elements.

This theoretical benchmark is important for other proposed clocks based on electric-quadrupole transitions in Cf^{15+} and Cf^{17+} [7]. The uncertainty of predictions for clock transitions in these ions is largely dominated by the effect of triple excitations in the coupled-cluster part of the computation, which is tested in this Letter.

Experiment—We laser cool single $^{224}\text{Ra}^+$ (3.6 d half-life) ions in a linear Paul trap with rf electrodes separated by 6 mm and end cap electrodes separated by 15 mm, described in Ref. [8]. The trap is in a vacuum chamber with a background pressure of 5×10^{-11} Torr measured with an ion gauge.

Lifetime measurements were initially attempted with $^{226}\text{Ra}^+$ (1600 yr half-life) in the same ion trap with a background pressure of 3×10^{-10} Torr. The pressure was likely limited by ^{222}Rn (3.8 d half-life) which was generated by the decay of the ^{226}Ra source (10 μCi). The measured lifetimes were systematically shifted up, probably from collisions with ^{222}Rn and trapped ions loaded from ionizing radiation. We tested the strength of the background ionizing radiation by successfully loading Sr^+ from a Sr atomic beam without photoionization light. These collisional effects were reduced by using $^{224}\text{Ra}^+$, which decays to ^{220}Rn , which has a relatively short 55.6 s half-life. The $^{224}\text{Ra}^+$ was loaded via photoionization from a ^{224}Ra atomic beam generated from a ^{228}Th source (25 μCi) [8].

The measurement pulse sequences consist of optical pumping to the target D state, a variable delay time in the dark, and state detection; see Figs. 2(a) and 3(a). The measurements start with Doppler cooling and a state detection pulse (SD1) that confirms that the ion is cold and in a bright state. The ion scatters 468 nm photons when it is illuminated by the 468 and 1079 nm lasers and is in the $S_{1/2}$ or the $D_{3/2}$ “bright” states. A fraction of the scattered photons are collected on a photomultiplier tube. If the ion is in a bright state, on average 126 photons are detected during the 10 ms-long state detection. If the ion is in the $D_{5/2}$ “dark” state, on average only 9.5 photons are detected from background scattered light. Before the variable delay, we set a detection threshold of 35 photon counts to determine the ion’s state. The dark state probability after the variable delay is determined using the maximum likelihood technique [9].

For the $D_{5/2}$ lifetime measurement, the cleanout or state preparation (SP) might fail, in which case we reject measurements where SD1 is dark or SD2 is bright. We fit the data, see Fig. 2(b), to an exponential decay, $p = ae^{-t/\tau_5}$, where p is the $D_{5/2}$ state population, a is the amplitude, and τ_5 is the lifetime of the $D_{5/2}$ state. The fit gives $1/\tau_5 = 3.284(14) \text{ s}^{-1}$.

Because both the $D_{3/2}$ and $S_{1/2}$ states are bright states, for the $D_{3/2}$ lifetime measurement we apply a 0.5 ms 708 nm pulse (SP2) after the delay to optically pump 10.930(13)% of the $D_{3/2}$ state population to the $D_{5/2}$ state through the $P_{3/2}$ state [9]. We reject measurements where SD1 is dark. The data is fit to an exponential [see Fig. 3(b)], which gives $1/\tau_3 = 1.54(2) \text{ s}^{-1}$.

Elastic and inelastic background gas collisions are the leading cause of systematic uncertainties for both lifetime measurements. Elastic collisions increase the kinetic energy of the ion, which can Doppler broaden transitions or remove the ion from the fiducial region, reducing the ion’s photon scattering rate during state detection and shifting up the measured lifetimes. We measure elastic collision rates by preparing the ion in the $S_{1/2}$ state and measuring the bright state probability versus delay time.

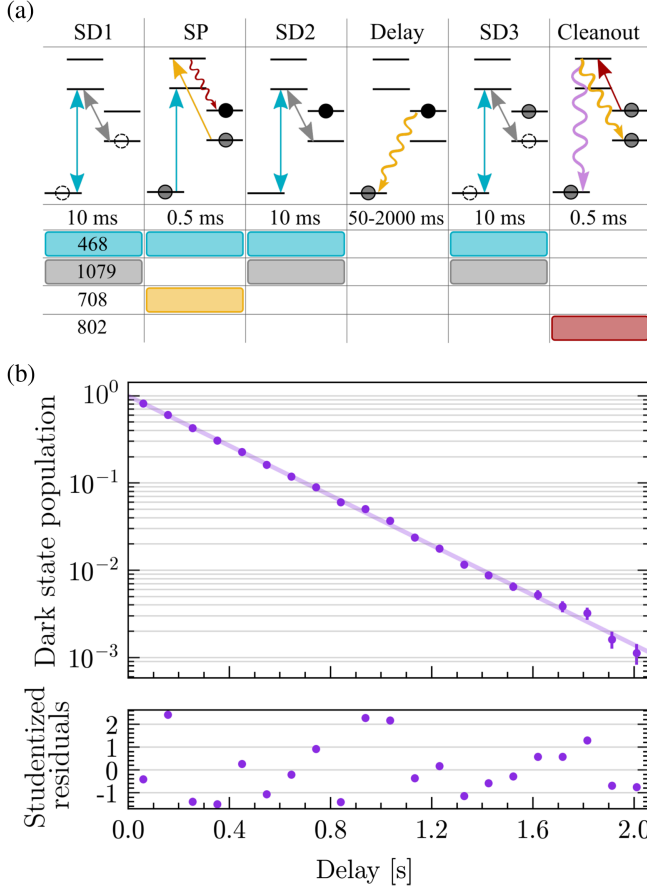


FIG. 2. (a) $6d^2D_{5/2}$ state lifetime measurement pulse sequence, and (b) measured dark state population fit to exponential decay with $\chi^2_\nu = 1.56$.

The measured elastic collision rate, $1.1(3) \times 10^{-4} \text{ s}^{-1}$ at $5 \times 10^{-11} \text{ Torr}$, shifts the $D_{5/2}$ and $D_{3/2}$ state decay rates down by $7.3(1.9) \times 10^{-3} \text{ s}^{-1}$ and $1.2(3) \times 10^{-2} \text{ s}^{-1}$, respectively.

Fine structure mixing occurs when inelastic collisions transfer population between the $D_{3/2}$ and $D_{5/2}$ states. The transfer rate is r_{53} from $D_{5/2}$ to $D_{3/2}$ and r_{35} for the reverse process. For low collision rates we make the approximation $r_{35} \rightarrow 0$ ($r_{53} \rightarrow 0$) when the ion is initialized in the $D_{5/2}$ ($D_{3/2}$) state [13]. Inelastic collisions can also quench the ion to its electronic ground state. It is reasonable to assume that the quenching rate, r_q , is the same for both D states [14].

For the $D_{5/2}$ state, inelastic collisions shift the decay rate by $r_{53} + r_q$. To measure $r_{53} + r_q$, we made two $D_{5/2}$ lifetime measurements at elevated pressures, $1.1 \times 10^{-10} \text{ Torr}$ and $2.2 \times 10^{-10} \text{ Torr}$, and obtain $r_{53} + r_q = 1(17) \times 10^7 \text{ s}^{-1} \text{ Torr}^{-1}$ from a linear fit to the decay rate versus pressure. This shifts the $D_{5/2}$ state decay rate up by $6(85) \times 10^{-4} \text{ s}^{-1}$ at $5 \times 10^{-11} \text{ Torr}$.

For the $D_{3/2}$ state, given our state detection scheme, any population transferred to the $D_{5/2}$ state contributes to the dark state probability. Therefore, a separate measurement

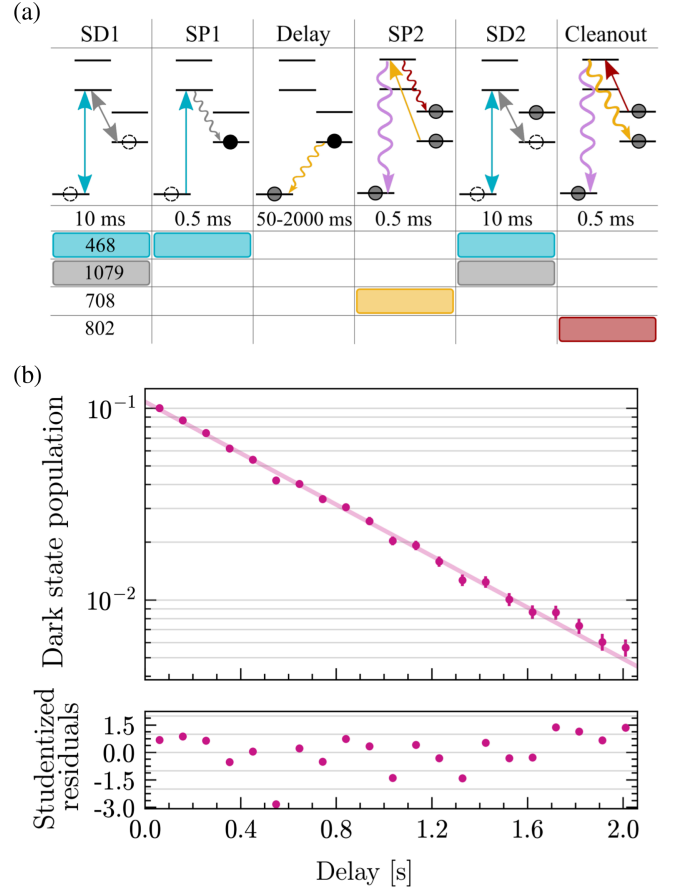


FIG. 3. (a) $6d^2D_{3/2}$ state lifetime measurement pulse sequence, and (b) measured dark state population fit to exponential decay with $\chi^2_\nu = 1.11$.

of r_{35} is needed to calculate the $D_{3/2}$ state decay rate shift due to fine structure mixing. We measure $r_{35} = 1(2) \times 10^{-4} \text{ s}^{-1}$ at $5 \times 10^{-11} \text{ Torr}$, which shifts the $D_{3/2}$ state decay rate down by $3(6) \times 10^{-4} \text{ s}^{-1}$ [13]. Instead of measuring the quenching rate with additional $D_{3/2}$ lifetime measurements at elevated pressures, we bound the corresponding uncertainty with $8.5 \times 10^{-3} \text{ s}^{-1}$, which is the combined $r_{53} + r_q$ uncertainty.

Systematic uncertainties with smaller effects are discussed in Supplemental Material [13]. Accounting for the shifts and uncertainties summarized in Table I, the $D_{5/2}$ state decay rate is $3.291(17) \text{ s}^{-1}$, giving a $303.8(1.5) \text{ ms}$ lifetime, and the $D_{3/2}$ state decay rate is $1.56(2) \text{ s}^{-1}$, giving a $642(9) \text{ ms}$ lifetime.

Theory—We consider Ra^+ to be a monovalent ion and construct the finite basis set of one-particle orbitals in the V^{N-1} approximation within the framework of the Dirac-Hartree-Fock (DHF) approach. The Breit interaction and quantum electrodynamical (QED) corrections are also taken into account [15].

We use the coupled-cluster single double triple (CCSDT) method, in which the coupled-cluster equations are solved

TABLE I. Shifts and uncertainties (in 10^{-3} s^{-1}) for the $6d \text{ } ^2\text{D}_{5/2}$ and $6d \text{ } ^2\text{D}_{3/2}$ state decay rates.

Source	$6d \text{ } ^2\text{D}_{5/2}$		$6d \text{ } ^2\text{D}_{3/2}$	
	Shift	Uncertainty	Shift	Uncertainty
Statistical	—	14	—	20
Elastic collisions	7.3	1.9	12	3
Inelastic collisions	−0.6	8.5	0.3	8.6
Max. likelihood	—	0.09	—	0.06
Thermal radiation	−0.017	0.005	0.05	0.01
Total	7	17	10	20

iteratively, including the core and valence triple excitations [2]. In the equations for single and double cluster amplitudes, the sums in excited states were carried out with 45 basis orbitals with orbital quantum number $l \leq 6$. In the equations for valence triples, we allowed the excitations of core electrons from the $[3s - 6p]$ shells; the sums in excited states were carried out with 32 basis orbitals with $l \leq 5$.

For an iterative solution of the equations for the core triples, more restrictions were applied due to drastically increased computational time. We solved these equations by allowing the core excitations from the $[4s - 6p]$ core shells, the maximal orbital quantum number l of all excited orbitals was equal to four, and the largest principal quantum number of the virtual orbitals where excitations were allowed was 22. These restrictions balance the enormous computational resources required for such a complete inclusion of the triple excitations with the need for high accuracy. We have verified that the present restrictions of these parameters give sufficient numerical accuracy by performing several computations with a different number of included core shells and virtual orbitals.

We started by calculating the removal energies of the low-lying states. The results of several increasing precision computations, as well as three additional corrections, are presented in Table II. The lowest order DHF excitation energies are labeled “DHF.” We then perform the calculation within the framework of the linearized coupled-cluster single double (LCCSD) approximation. The most complete calculation included the NL terms and the valence and core triple excitations. We designate this calculation as CCSDT.

We also list the QED corrections (ΔE_{QED}) and the corrections due to the Breit interaction (ΔE_{Breit}) and basis extrapolation (ΔE_{extrap}). The latter is the contribution of the higher ($l > 6$) partial waves. It was determined based on previous studies [17]. The total values, shown in the row labeled “ E_{total} ,” are determined as the CCSDT values plus the three corrections. The difference between the total and experimental values is given (in percent) in the row labeled “Difference (%)”.

To illustrate a consistent improvement in the results when we add different corrections, we present the differences between the theoretical and experimental values obtained at each stage of the calculation in the lower panel of Table II. Comparing Δ_{total} with the experimental values [16], we see a very good agreement for the removal energies of the $7s \text{ } ^2\text{S}_{1/2}$ and $6p \text{ } ^2\text{P}_{1/2,3/2}$ states. A slightly larger difference between theory and experiment for the $6d \text{ } ^2\text{D}_{3/2,5/2}$ states is likely attributed to the nonlinear triple terms contribution omitted in our calculation as well as a larger contribution of the higher partial waves for these states. But even for $6d \text{ } ^2\text{D}_{3/2,5/2}$, the agreement with the experiment, at the level of 0.1%, is exceptionally good for such a complicated system.

 TABLE II. The removal energies of the low-lying states (in cm^{-1}) in different approximations discussed in the text are presented. The theoretical total and experimental results are given in the rows E_{total} and E_{expt} . The difference between E_{total} and E_{expt} [16] is presented (in percent) in the row labeled “Difference (%)” $\Delta_X \equiv E_X - E_{\text{expt}}$.

	$7s \text{ } ^2\text{S}_{1/2}$	$6d \text{ } ^2\text{D}_{3/2}$	$6d \text{ } ^2\text{D}_{5/2}$	$6p \text{ } ^2\text{P}_{1/2}$	$6p \text{ } ^2\text{P}_{3/2}$
E_{DHF}	75898	62356	61593	56878	52906
E_{LCCSD}	82508	70186	68436	60865	5584
E_{CCSDT}	81894	69584	67926	60493	55597
ΔE_{Breit}	−19	62	87	−54	−13
ΔE_{QED}	−74	66	54	13	7
ΔE_{extrap}	37	127	115	26	22
E_{total}	81 838	69 839	68 182	60 478	55 613
E_{expt} [16]	81 843	69 758	68 100	60 491	55 634
Difference (%)	−0.00	0.12	0.12	−0.02	−0.04
Δ_{DHF}	−5945	−7402	−6507	−3613	−2728
Δ_{LCCSD}	666	438	336	374	260
Δ_{CCSDT}	51	−174	−174	2	−37
Δ_{total}	−4	80	82	−13	−21

TABLE III. Reduced MEs $\langle 7s^2S_{1/2} || Q || 6d^2D_{3/2,5/2} \rangle$ obtained in the DHF, LCCSD, and CCSDT approximations (see text for details) are presented in $|e|a_0^2$, where a_0 is the Bohr radius. The uncertainties of the final values are given in parentheses.

	$\langle ^2S_{1/2} Q ^2D_{3/2} \rangle$	$\langle ^2S_{1/2} Q ^2D_{5/2} \rangle$
DHF	17.26	21.77
LCCSD	14.59	18.69
$\Delta(\text{NL})$	0.16	0.19
$\Delta(\text{Tr})$	-0.11	-0.11
$\Delta(\text{Breit \& QED})$	-0.02	-0.03
$\Delta(l=7)$	-0.02	-0.02
Final CCSDT	14.60(7)	18.72(9)
Ref. [18]	14.74(15)	18.86(17)
Ref. [19]	14.87(7)	19.04(5)

In Table III, we present the reduced matrix elements (MEs) of the electric-quadrupole moment operator, $\langle 7s^2S_{1/2} || Q || 6d^2D_{3/2,5/2} \rangle$, calculated in different approximations discussed above. The results displayed in the rows labeled “DHF” and “LCCSD” are obtained in the DHF and LCCSD approximations, respectively. Rows 3–6 give different corrections. Corrections resulting from NL terms and triples are listed in rows labeled “ $\Delta(\text{NL})$ ” and “ $\Delta(\text{Tr})$.” The Breit interaction and QED corrections are small, and we present their total value in the row labeled “ $\Delta(\text{Breit \& QED})$ ”. To estimate the contribution of partial waves with $l > 6$, we reconstructed the basis set, including partial waves with the orbital quantum number up to $l = 7$. The difference between the LCCSD values of the MEs obtained for the basis sets with $l_{\max} = 7$ and $l_{\max} = 6$ is given in the row labeled “ $\Delta(l=7)$.” The final (recommended) values are obtained as the sum of the LCCSD values plus all corrections listed in rows 3–6. We note that these corrections essentially cancel each other out and all of them have to be included in the precision computation.

There are several sources of uncertainties in the final values of the MEs, such as small residual numerical inaccuracy in the calculation of the correlation corrections, omission of the NL terms in the triple equations, and a contribution from partial waves with $l > 7$. Based on an estimate of possible contributions to the MEs from these effects, we assign uncertainties at the level of 0.5% to the final values.

Using these values of the MEs, we calculated the electric-quadrupole and magnetic-dipole transition rates W , and lifetimes of the $^2D_{3/2}$ and $^2D_{5/2}$ states. We note that $W(^2D_{5/2} \rightarrow ^2D_{3/2})$ is completely dominated by the $M1$ transition. The contribution of the electric-quadrupole transition $^2D_{5/2} \rightarrow ^2D_{3/2}$ is very small, and we neglect it. We find results (see Table IV) that are in good agreement with those obtained in [18].

Using the final values of the MEs given in Table III we find the ratio

TABLE IV. Transition rates (W) of the electric-quadrupole $^2D_{3/2,5/2} \rightarrow ^2S_{1/2}$ and the magnetic-dipole $^2D_{5/2} \rightarrow ^2D_{3/2}$ transitions and the lifetimes (τ) of the $^2D_{3/2}$ and $^2D_{5/2}$ states are presented. The uncertainties are given in parentheses.

			This work	Ref. [18]	Ref. [19]
$W(\text{s}^{-1})$	$E2$	$^2D_{3/2} \rightarrow ^2S_{1/2}$	1.539(15)	1.568	
	$E2$	$^2D_{5/2} \rightarrow ^2S_{1/2}$	3.207(32)	3.255	
	$M1$	$^2D_{5/2} \rightarrow ^2D_{3/2}$	0.049	0.049	
$\tau(\text{ms})$		$^2D_{3/2}$	650(7)	638(10)	627(4)
		$^2D_{5/2}$	307(3)	303(4)	297(4)

$$R_{E2} \equiv \frac{\langle ^2S_{1/2} || Q || ^2D_{5/2} \rangle}{\langle ^2S_{1/2} || Q || ^2D_{3/2} \rangle} = 1.282(3). \quad (1)$$

We estimate the uncertainty of this ratio as the largest difference between the values of R_{E2} obtained in different approximations. Using Eq. (1), we find the ratio of the transition rates,

$$R_{W2} \equiv \frac{W(^2D_{5/2} \rightarrow ^2S_{1/2})}{W(^2D_{3/2} \rightarrow ^2S_{1/2})} \approx 2.084(6). \quad (2)$$

Since the uncertainties of the transition energies are negligible compared to the uncertainty of R_{E2} , we estimate the absolute uncertainty of R_{W2} as $\Delta R_{W2} \approx 2(\Delta R_{E2}) = 0.006$.

A comparison of theoretical values and measured lifetimes is shown in Fig. 4. No uncertainty is assigned to the reported lifetimes in [20]. We also note that the uncertainties reported in [21] appear to be underestimated. For example, Ref. [21] reported $\langle ^2S_{1/2} || Q || ^2D_{3/2} \rangle = 14.687(42)$ a.u. calculated in the framework of the CCSD method. Table III of this Letter shows that the triple excitations correction for $\langle ^2S_{1/2} || Q || ^2D_{3/2} \rangle$, which is omitted in their computation, is -0.11 , almost 3 times larger than the total uncertainty of 0.04 assigned in Ref. [21].

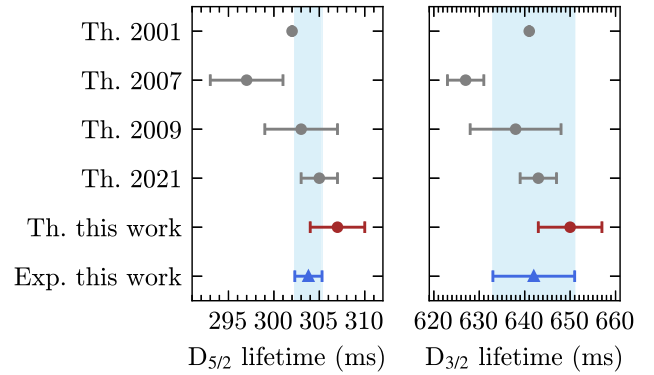


FIG. 4. Comparison of the measured $D_{5/2}$ state and $D_{3/2}$ state lifetimes with theoretical calculations in this and previous works [18–21].

Conclusion—We have measured and calculated the lifetimes of the $6d\ ^2D_{3/2}$ and $6d\ ^2D_{5/2}$ states of Ra^+ . This Letter presents the first tests of the CCSDT method for transition properties. The long lifetimes of the $6d\ ^2D_{5/2}$ and the $6d\ ^2D_{3/2}$ states support the prospect of using $7s\ ^2S_{1/2} \rightarrow 6d\ ^2D_{5/2}$ and $7s\ ^2S_{1/2} \rightarrow 6d\ ^2D_{3/2}$ E2 clock transitions for future frequency standards with the Ra^+ ion.

Acknowledgments—The authors thank H. Häffner for useful discussions. H.L. was supported by ONR Grant No. N00014-21-1-2597 and M.F. was supported by DOE Award No. DE-SC0022034. H.D., S.K., R.K., R.A.R., A.S., M.B., C.A.H. and A.M.J. were supported by the Heising-Simons Foundation Award No. 2022-4066, the W.M. Keck Foundation, NIST Award No. 60NANB21D185, NSF NRT Grant No. 2152201, the Eddleman Center, the Noyce Initiative, and NSF Grants No. 2326810, No. 2146555, and No. 1912665. The isotope used in this research was supplied by the U.S. Department of Energy Isotope Program, managed by the Office of Isotope R&D and Production. The theoretical work was supported by the U.S. NSF Grant No. PHY-2309254, U.S. Office of Naval Research Grants No. N00014-20-1-2513, No. N000142512105 and the European Research Council (ERC) under the Horizon 2020 Research and Innovation Program of the European Union (Grant Agreement No. 856415). The calculations in this work were done through the use of Information Technologies resources at the University of Delaware, specifically the high-performance Caviness and DARWIN computer clusters.

Data availability—The data that support the findings of this Letter are openly available [22]. The data supporting the theoretical results are available in the Letter.

[1] G. Arrowsmith-Kron *et al.*, *Rep. Prog. Phys.* **87**, 084301 (2024).
 [2] S. G. Porsev, M. S. Safronova, and M. G. Kozlov, *Phys. Rev. Lett.* **127**, 253001 (2021).
 [3] O. O. Versolato, L. W. Wansbeek, G. S. Giri, J. E. v. d. Berg, D. J. v. d. Hoek, K. Jungmann, W. L. Kruithof, C. J. G. Onderwater, B. K. Sahoo, B. Santra, P. D. Shidling, R. G. E. Timmermans, L. Willmann, and H. W. Wilschut, *Hyperfine Interact.* **199**, 9 (2011).

[4] C. A. Holliman, M. Fan, A. Contractor, S. M. Brewer, and A. M. Jayich, *Phys. Rev. Lett.* **128**, 033202 (2022).
 [5] S. M. Brewer, J.-S. Chen, A. M. Hankin, E. R. Clements, C. W. Chou, D. J. Wineland, D. B. Hume, and D. R. Leibrandt, *Phys. Rev. Lett.* **123**, 033201 (2019).
 [6] C. A. Holliman, M. Fan, and A. M. Jayich, in *Quantum Sensing, Imaging, and Precision Metrology* (SPIE, Bellingham, WA, 2023), Vol. PC12447, p. PC124470C.
 [7] S. G. Porsev, U. I. Safronova, M. S. Safronova, P. O. Schmidt, A. I. Bondarev, M. G. Kozlov, I. I. Tupitsyn, and C. Cheung, *Phys. Rev. A* **102**, 012802 (2020).
 [8] M. Fan, R. A. Ready, H. Li, S. Kofford, R. Kwapisz, C. A. Holliman, M. S. Ladabaum, A. N. Gaiser, J. R. Griswold, and A. M. Jayich, *Phys. Rev. Res.* **5**, 043201 (2023).
 [9] M. Fan, C. A. Holliman, S. G. Porsev, M. S. Safronova, and A. M. Jayich, *Phys. Rev. A* **100**, 062504 (2019).
 [10] M. Fan, C. A. Holliman, A. L. Wang, and A. M. Jayich, *Phys. Rev. Lett.* **122**, 223001 (2019).
 [11] M. Fan, C. A. Holliman, A. Contractor, C. Zhang, S. F. Gebretsadkan, and A. M. Jayich, *Phys. Rev. A* **105**, 042801 (2022).
 [12] S. Kofford, H. Li, R. Kwapisz, R. A. Ready, A. Sawhney, O. C. Cheung, M. Fan, and A. M. Jayich, *Phys. Rev. A* **111**, 032802 (2025).
 [13] See Supplemental Material at <http://link.aps.org/supplemental/10.1103/5754-4cbv> for detailed discussions on systematics and analysis uncertainties.
 [14] N. Yu, W. Nagourney, and H. Dehmelt, *Phys. Rev. Lett.* **78**, 4898 (1997).
 [15] I. I. Tupitsyn, M. G. Kozlov, M. S. Safronova, V. M. Shabaev, and V. A. Dzuba, *Phys. Rev. Lett.* **117**, 253001 (2016).
 [16] A. Kramida, Yu. Ralchenko, and J. Reader (NIST ASD Team), *NIST Atomic Spectra Database (version 5.12)* (National Institute of Standards and Technology, Gaithersburg, MD, 2024), <https://physics.nist.gov/asd>.
 [17] S. G. Porsev, C. Cheung, M. S. Safronova, H. Bekker, N. H. Rehbehn, J. R. C. Lopez-Urrutia, and S. M. Brewer, *arXiv*: 2407.17610.
 [18] R. Pal, D. Jiang, M. S. Safronova, and U. I. Safronova, *Phys. Rev. A* **79**, 062505 (2009).
 [19] B. K. Sahoo, B. P. Das, R. K. Chaudhuri, D. Mukherjee, R. G. E. Timmermans, and K. Jungmann, *Phys. Rev. A* **76**, 040504(R) (2007).
 [20] V. A. Dzuba, V. V. Flambaum, and J. S. M. Ginges, *Phys. Rev. A* **63**, 062101 (2001).
 [21] F.-C. Li, H.-X. Qiao, Y.-B. Tang, and T.-Y. Shi, *J. Quant. Spectrosc. Radiat. Transfer* **274**, 107877 (2021).
 [22] H. Li, Zenodo (2025), 10.5281/zenodo.15795389.